Wheat and ryegrass biomass ashes as effective sorbents for metallic and organic pollutants from contaminated water in lab-engineered cartridge filtration system

Théo Guérin, Alina Ghinet, Marc Hossarte, Christophe Waterlot

Wheat and ryegrass biomass ashes as effective sorbents for metallic and organic pollutants from contaminated water in lab-engineered cartridge filtration system

Théo Guérin[1,2], Alina Ghinet[2,3,4], Marc Hossart[5], Christophe Waterlot[1,*]

[1] Univ. Lille, IMT Douai, Univ. Artois, Yncréa Hauts-de-France, ULR 4515 - LGCgE, Laboratoire de Génie Civil et géo-Environnement, F-59000 Lille, France

[2] Yncréa Hauts-de-France, Laboratory of Sustainable Chemistry and Health, Health & Environment Department, Team Sustainable Chemistry, Ecole des Hautes Etudes d'Ingénieur (HEI), UCLille, 13 rue de Toul, F-59046 Lille, France

[3] Univ. Lille, Inserm, CHU Lille, Institut Pasteur de Lille, U1167 - RID-AGE - Facteurs de risque et déterminants moléculaires des maladies liées au vieillissement, F-59000 Lille, France

[4] Faculty of Chemistry, Department of Organic Chemistry, 'Al. I. Cuza' University of Iasi, Bd. Carol I nr. 11, 700506 Iasi, Romania

[5] La Spiruline de Marc, 2 bis Grande Rue, 80560 Saint-Léger-lès-Authie

[*] Corresponding author: christophe.waterlot@yncrea.fr

Keywords: sorption; metal and emerging organic contaminant; numerical modelling, miscanthus biochar; ryegrass; wheat straw; cartridge filtration technology.

Abstract

Three plant biomasses (miscanthus, ryegrass and wheat) have been considered for the preparation of five different sorbents evaluated for their potential to sorb cadmium and lead and four emergent organic compounds (diclofenac, sulfamethoxazole, 17α-ethynylestradiol and triclosan) from artificially contaminated water. Lab-created cartridges were filled with each sorbent and all

experiments were systematically compared to activated charcoal Norit®. Results from activated charcoal, wheat straw and acidified wheat straw were supported by the Langmuir and Freundlich models. Wheat straw ashes were an excellent metal extractor that exceeded the potential of well-known activated charcoal. Acidified sorbents (wheat and ryegrass) were very effective in eliminating the selected emerging organic contaminants displaying equipotent or superior activity compared to activated charcoal. These results open the way for further *in natura* studies by proposing new biosource materials as new effective tools in the fight against water pollution.

Introduction

Chemical pollution has a major contribution in degrading water quality and so, a negative impact on human and environmental health. Human activities (*e.g.* industries, care institutions, animal farming) generate metal trace elements (MTE) and emerging organic contaminants (EOCs) which are spilled into natural water stream. This pollution is very problematic since pollutants accumulate rapidly and reach toxic concentrations for the environment and humans. Cadmium (Cd) and lead (Pb) are the most common toxic MTE since they are both carcinogenic, mutagenic and reprotoxic. EOCs are also a real concern (Lapworth et al., 2012). They include a wide array of different categories such as pharmaceutical compounds, pesticides or food additives. They have undesirable impacts on the environment and induce human health damages (Jean et al., 2012). They also generate microbial drug resistance (Andersson et al., 2012). Despite their lower concentration compared to MTE, they have a longer half-time life and persist in the environments in which they are found. Nowadays, the sewage treatment plants are not sufficiently effective to completely purify these contaminated waters. It is therefore crucial to find low-cost, sustainable and effective solutions to manage these pollutants and to clean water.

Research and technology have led to the discovery of diversified techniques for the removal of pollutants (Rodriguez-Narvaez et al., 2017). Among them, sorption is one of the most preferred mainly because it is economically viable whereas the other practices are much more expensive (Sophia et al., 2018). This technique consists in the use of materials which are able to sorb inorganic and organic pollutants in order to remove them from water. Activated charcoal (AC) is the most widely used

sorbent due to its efficiency and availability (Burakov et al., 2018). However, its cost remains a limiting factor for a large-scale applications. To overcome this main drawback, sorbents like zeolites, mineral clays, industrial solid wastes and nanostructured materials have been developed (Burakov et al., 2018) and new sorbents have recently been identified from crude or modified biomass (*e.g.* biochar, coffee grounds, biopolymers, agricultural waste) (Bhatnagar et al., 2015; Zhou et al., 2016; Janus et al., 2017; Ahsan et al., 2018; Luo et al., 2018; Naga Babu et al., 2018; Tursi et al., 2018; Żółtowska-Aksamitowska et al., 2018; Fernández-López et al., 2019; Fu et al., 2020 ;).

Since the end of the 20th century, several studies have been carried out on ash-based sorbents. Ashes are secondary products generated in very large quantities by industries and they are often considered as a waste. From an ecological and economical point of view, they may constitute sorbents of choice. In this context, Gupta and coworkers (2000, 2002, 2003) tested the efficiency of bagasse fly ashes in the removal of dyes, lindane, malathion, Cd and copper from contaminated water (Gupta and Ali, 2000). More recently, research efforts have been focused on ash-based sorbents from *Citrullus colocynthis* (Qasemi et al., 2018), coir pith (Bahar et al., 2018) or Jamun (*Syzygium cumini*) leaves (Tirkey et al., 2018) in order to respectively remove phenol, arsenic and fluoride from contaminated water.

To tackle the complex problem of contaminated water, new low-cost and sustainable sorbents were developed from two different biomass ashes (*Lolium perenne* L. and *Triticum aestivum* L.) with or without acidification. Because MTE contamination and EOCs are both extremely problematic, the retention performance of representative molecules selected from the two classes of pollutants was evaluated on acidified and non-acicidified ashes. The sorption tests reported herein covered the use Cd, Pb and four poorly studied EOCs: a nonsteroidal anti-inflammatory drug (diclofenac, DCF; Bonnefille et al., 2018), an antibiotic (sulfamethoxazole, SFX; Wang et al., 2018), a female hormone (17α-ethinylestradiol, EE2; Jackson et al., 2019) and an endocrine disruptor (triclosan, TCL; Thomaidi et al., 2017; Zaltauskaite et al., 2018). The chemical structure, selected chemical and physical properties as well as pictograms of these compounds are described in Table 1.

Materials and Methods

Organic and inorganic pollutants

All chemicals and reagents used were of analytical grade. Sulfamethoxazole (SFX), triclosan (TCL) and 17α-ethynylestradiol (EE2) were obtained from Sigma Aldrich and diclofenac (DCF) from TCI Chemicals. These organic pollutants were dissolved in a mixture of ultra-pure water (18 MΩ-cm at 25 °C) and absolute ethanol (purchased from Carlo Erba Reagents) as follows: 50/50 EtOH/H_2O for EE2, 40/60 EtOH/H_2O for DCF, 30/70 EtOH/H_2O for TCL and 100 H_2O for SFX. The Cd and Pb metal stock solutions at 1000 mg L^{-1} in 2% HNO_3 (Chemical Products for Analysis, Association Corporation Standard Distribution, C.P.A. groupe A.C.S.D., Voisins le Bretonneux, France) were used for the preparation of diluted metal solutions with ultra-pure water.

Solid support

Activated Charcoal (AC) Norit SA-2 from Acros Organics was chosen as the reference sorbent. The properties of this material are given hereafter: iodine number: 850; specific surface area: 950 m^2 g^{-1}; apparent density: 460 kg m^{-3}; particle size D_{10} (µm): 3; particle size D_{50} (µm): 20; particle size D_{90} (µm): 140; ash content (% mass): 9. The first investigated sorbent was a miscanthus biochar (MB), described in detail in Janus et al. (2017). Four additional sorbents were produced for the current study using shoots of ryegrass (*Lolium perenne* L.) and wheat straw (*Triticum aestivum* L.). Two sorbents were obtained from crude ashes of ryegrass (R) and wheat straw (WS) and the others resulted from an acidic treatment of the respective crude ashes, named AR and AWS, respectively. The shoots of ryegrass were harvested in a private lawn without specificity. They were transformed into ashes in a muffle furnace (Nabertherm P330, Lilienthal, Germany) under air flow using the following temperature program: (i) 20 to 250 °C in 30 min, (ii) 250 °C for 1 hour, (iii) 250 to 500 °C in 2 hours and (iv) 500 °C for 8 hours. The wheat straw ashes were obtained from a spirulina powder producer (La Spiruline de Marc, Saint-Léger-lès-Authie, France). The acidification of ashes was conducted using a 2M HCl aqueous solution with a weight ratio ashes/HCl: 1/10. The mixture was stirred at 70 °C for 2 hours and then, filtered. The resulting solid was then dried at 105 °C for 16 hours.

110 ***Mineralisation***

111 300 mg of ashes (R, WS, AR and AWS) were added to a mixture of 37% HCl (4.5mL) and 70%
112 HNO_3 (1.5 mL). The resulting suspension was heated at 120 °C for 90 min in a digester (HotBlock™
113 Environmental Express®SC100, Charleston, USA). Ultra-pure water was then added until reaching a
114 total volume of 25 mL and was then filtered over an acetate Millipore membrane (0.45 µm porosity).
115 The concentrations of Cd and Pb were measured by flame atomic absorption spectrometry (FAAS;
116 AA-6800 Shimadzu, Tokyo, Japan) following the recommendation described in the literature
117 (Waterlot and Douay, 2009; Savio et al., 2010). The limits of detection (LD) of Cd and Pb were 2.1 µg
118 L^{-1} and 41 µg L^{-1}, respectively (Waterlot and Hechelski, 2019). It is worth mentioning that the
119 concentrations of Cd and Pb in R, WS, AR and AWS were below the limit of detection.
120
121 ***Sorption experiments***

122 With the aim of getting as close as possible to an industrially exploitable process, the adsorption
123 experiments were carried out by eluting the contaminated solutions on lab-made cartridges (Redisep
124 Rf column with a diameter of 1.5 cm from Teledyne Technologies Inc.) filled with ashes from the
125 selected solid supports (AC, MB, R, WS, AR or AWS; Figure 1). All experiments were conducted
126 under normal temperature and pressure (NTP) conditions (20 °C; 1 atm). After adding and packing
127 200 mg of cotton, 1000 mg of sorbent were introduced in the column. Then, 25 mL of artificially
128 contaminated water (20 mg pollutant L^{-1}) were added into the column. After the filtration (30 min
129 were necessary for the complete elution), the resulting solutions were analysed in order to select
130 sorbents with the best retention capacity. This capacity was then defined using solutions of different
131 concentrations (from 10 mg L^{-1} to 1000 mg L^{-1}) on 250 mg of sorbent by means of Freundlich and
132 Langmuir models. The concentrations of Cd and Pb in the contaminated water samples before and
133 after filtration were measured by FAAS.
134
135 ***EOCs and PAHs analyses***

136 EOCs (TCL, SFX, EE2 and DCL) were analysed on a Shimadzu UFLC system (Prominence,
137 Shimadzu, Tokyo, Japan) equipped with a LC-20AD quaternary pump, an automatic refrigerated

sample injector (SIL-20AC), a thermostatted column compartment (CTO-20AC), a five-channel online degasser (DGU-20A5R) and a diode array detector (SPD-M20A). All material was linked through a CBM-20 controller monitored by the LabSolutions® software (Shimadzu) to acquire and process the chromatograms. The column used in the current study was a Kinetex®-C18 column (250 mm x 4.6 mm) packed with 5 µm core-shell particles (Phenomenex, Le Pecq, France). The calibration curves were obtained using solutions of single organic pollutant (SFX, EE2, TCL or DCL) at the following concentrations: 0.1, 0.2, 0.5, 0.8, 1, 2, 5, 8, 10, 15 and 20 mg L^{-1}. The limits of detection (LD) and quantification (LQ) were determined from the ratios signal-to-noise of 3 and 10, respectively (Sun et al., 1998; Santos et al., 2007). A list of selected parameters was given in Table 2.

Due to the potential release of polycyclic aromatic hydrocarbons (PAHs) from the biochar to the purified solutions (Janus et al., 2017), naphthalene, fluorene, acenaphthene, phenanthrene, anthracene, fluoranthene, pyrene, chrysene, benzo[*a*]anthracene, benzo[*b*]fluoranthene, benzo[*k*]fluoranthene, benzo[*a*]pyrene, dibenzo[*a,h*]anthracene, benzo[*g,h,i*]perylene, and indeno[1,2,3-*c,d*]pyrenes were analysed in filtrates according to the procedure described in previous studies (Goulas et al., 2015; Waterlot and Goulas, 2016). The chromatographic system was fitted with an FLD (RF-20A) set at varying excitation and emission wavelengths. A standard solution (EPA-610 OekanalR; Sigma-Aldrich, Saint-Quentin Fallavier, France) of these 15 EPA PAHs was diluted to a concentration of 500 g L^{-1} with acetonitrile (HPLC quality, purity >99.9%, ChromasolvR; Sigma–Aldrich) as working solution.

Results and discussion

Preliminary results obtained with miscanthus biochar, shoots of ryegrass and wheat straw

Miscanthus biochar (MB)

Janus et al. (2017) showed that MB (0.5 g) was able to sorb Cb (78-96%) and Pb (98-99%) from solution at 0.06 mg Cd kg^{-1} and at 4 mg Pb kg^{-1} in batch conditions. These results have been recently confirmed by Boni et al (2018, 2020). As indicated in Table 3, MB was efficient to sorb Pb (99.7%) from the stock solution at 20 mg L^{-1} (25 mL) using the newly engineered cartridge filtration system

(Figure 1). In contrast, Cd sorption was very low (15.3%). This means that only 76.5 mg of Cd were adsorbed per g of MB support. As shown in Table 3, this support was not effective either in the retention of EE2, SFX and DCF (respectively 5%, 0% and 0%). Contrariwise, 87.7% of the initial TCL concentration was retained on the MB support, which was produced at 600 °C (Janus et al., 2017). In their review, Tomczyk et al. (2020) reported the retention of compounds like phenolic acid and carboxyl functions when biochars were produced up to 480 °C. Above this temperature, the authors revealed a decrease of the cation exchange capacity (CEC) and the formation of aromatic carbon, improving π-π interactions with aromatic pollutants. These both phenomena could explain why TCL was the only retained compound among the organic pollutants studied. Drawbacks in using biochars as sorbents were related to the release of PAHs as described in literature (Liu et al., 2019; Wang et al., 2019). In the current study, fluorene, acenaphthene, phenanthrene and anthracene were detected in solutions after their filtration on biochars. Concentrations of these PAHs were 28.35 ± 1.15 µg L^{-1}, 17.25 ± 8.56 µg L^{-1}, 6.01 ± 2.08 µg L^{-1}, 4.00 ± 1.29 µg L^{-1}, respectively.

Shoots of ryegrass and wheat straw

Ashes from ryegrass (R) and wheat straw (WS) were used as sorbents as well as their respective acidified forms (AR, AWS). These supports were compared to the activated charcoal (AC) support, used as reference. The first experiments were conducted with pollutants in solution at 20 mg L^{-1} using 1 g of sorbent. As shown in Table 4, the MTE concentrations measured in the filtrates were below 0.05 mg L^{-1} meaning that AC has retained 99.96% and 99.75% of Cd and Pb from the initial solution. Similar results were obtained with ashes from ryegrass (R) and wheat straw (WS) since the retention of Cd was 99.71% and 99.99%, respectively and 99.50% and 99.92%, respectively for Pb. In contrast, the efficiency of these two supports after their acidification (AR, AWS) dramatically decreased, making it impossible to use them for the intended purpose.

Reference support (AC), non-acidified and acidified supports from biomass were also used in the retention of organic pollutants. 25 mL of each solution (TCL, SFX, EE2 and DCF at 20 mg L^{-1}) were passed through the studied sorbents (1 g; Figure 1) and the resulting filtrates were analysed. Depending on the organic pollutants, the retention varied from 97.45% to 99.99% by using activated charcoal (Table 5). This result is not surprising since activated charcoal was described as an effective

support for the removal of emerging pollutants like pesticides, pharmaceuticals, endocrine disrupting chemicals due to the presence of various mechanisms (π-π interactions, hydrogen bonds and electron donor-acceptor complex formation) and chemical functions (Jeirani et al., 2017). Ashes from ryegrass didn't retain any of the studied organic pollutants and the retention of these pollutants using ashes from WS was very low, ranging from 0% to 30.43%. Acidified supports were more appropriate to the retention of TCL, SFX and DCF since the percentages of retention were in the range of 86.55% to 99.99%. The best results were obtained with ashes AWS since the concentration of TCL, SFX and DCF in filtrates were below the limits of detection. Regarding EE2, this support is less effective than AC since the achieved retention was only 43.83% *versus* 97.46% (Table 5). As shown in Table 1, the chemical composition, molecular structure, functional groups, dipole moment and lipophilicity of EE2 are very different from those of TCL, SFX and DCF. On the other hand, the hydrophobic property of EE2 is higher than that of the three other compounds. Consequently, the hydrophobicity partitioning does not seem to be the main sorption mechanism in this case. This result correlated well with the studies conducted by several authors which highlighted that this mechanism was dominant on biochar, activated charcoal, sediment and soil (Sun et al., 2012; Li et al., 2013; Guo et al., 2013; Trigo et al., 2014).

Sorption Isotherms and modelling

The sorption capacity was evaluated for the reference support (AC) and the best biomass supports (WS and AWS) using Cd and TCL as metal and organic pollutants. Experiments were conducted in three independent experiments using the system described in Figure 1 in which 250 mg of solid support were preliminary added to the addition of contaminated water (25 mL).

Cd isotherms were presented in Figure 2A. Excellent linearity was obtained up to 350 mg L^{-1} using WS (R^2 = 0.999) and 200 mg L^{-1} for CA (R^2 = 0.996). In the current experimental conditions, the two sorption curves clearly highlighted a best capacity of Cd sorption of ashes from wheat straw since (i) the slope of the curve obtained for AC is the lowest and (ii) Qe value is lower than that obtained with WS.

Sorption isotherms of TCL using AC and acidified ashes from wheat straw (AWS) are presented in Figure 2B. Although AWS support was more efficient in the retention of TCL between 10 mg L^{-1} and 60 mg L^{-1} than AC, the sorption capacity of both supports was quite similar at 80 mg L^{-1} (Qe = 5.04 mg g^{-1} for AC and Qe = 4.76 mg g^{-1} for AWS). It is worth noting that the maximum sorption capacity of AC was at 100 mg TCL L^{-1}.

Langmuir and Freundlich models were used for modeling adsorption data (Hamdaoui and Naffrechoux., 2007).

Langmuir model

Langmuir isotherm model suggests that sorption occurs as monolayer exposure on homogeneous surface comprising energetically equivalent sites without any steric hindrance and lateral interactions between sorbed molecules. The energy of sorption is constant and is independent on the degree of occupation of the sorbent active centers. One of the linear expressions of the Langmuir isotherm is given by the equation (1).

$$1/q_e = 1/C_e b q_m + 1/q_m, \qquad (1)$$

where q_e is the amount of pollutant adsorbed per g of support (mg g^{-1}), C_e represents the equilibrium concentration of the adsorbate material (mg L^{-1}), q_m is the maximum adsorption capacity (mg g^{-1}) and b is a constant associated to the free energy of adsorption (L mg^{-1}).

Langmuir isotherms of Cd and TCL were plotted in Figures 3A and 3B, respectively. Very good correlation coefficients were obtained for each modality, ranging from 0.975 to 0.996 (Table 6). From the linear equation, the Langmuir constants (b and q_m) were calculated (Table 6). The maximal sorption capacities of SW/ASW were 2.6 and 3.6-fold higher than those of AC. On the other hand, for the two pollutants, b values for AC were slightly higher than those obtained for SW/ASW. These results indicated that the affinity of Cd and TCL for AC were slightly higher than for SW/ASW (Blázquez et al., 2012). This constant is very interesting since it can be expressed as a function of the Gibbs free energy according to the equation (2) (Djelloul 2014).

$$\mathrm{Ln}\,(1/b) = \Delta G^{\circ}/RT \qquad (2)$$

where ΔG° is the Gibbs free energy of the sorption reaction (J mol^{-1}), *b* is a constant associated to the free energy of adsorption (L mol^{-1}), T is the temperature (K) and R the universal gas constant (J mol^{-1} K^{-1}).

This Gibbs free energy is expressed by the equation (3).

$$\Delta G^{\circ} = - RT \ln b \qquad (3)$$

Numerical values of ΔG° were negative for both Cd and TCL on AC (-10.72 KJ mol^{-1} and -20.70 KJ mol^{-1}, respectively) as well as on WAS/AWS (-7.42 KJ mol^{-1} and -18.KJ mol^{-1}). In this regard, the adsorption processes onto AC and WS/AWS supports were found to be spontaneous.

As described by Hamdaoui and Naffrechoux (2007), the equilibrium parameter R_L was calculated following the equation (4).

$$R_L = 1/(1 + b*C_0) \qquad (4)$$

where C_0 is the initial concentration of the adsorbate in solution (mg L^{-1}) and *b* is a constant associated to the free energy of adsorption (L mg^{-1}). Depending of the value of the Hall parameter (R_L), the sorption can be defined as irreversible ($R_L = 0$), favourable ($0 < R_L < 1$), linear ($R_L = 1$) or unfavourable ($R_L > 1$).

Figure 4 shows the variation of the Hall parameter of Cd (Fig. 4A) and TCL (Fig. 4B) using the two supports studied. Whatever the initial concentration was, the R_L value ranged from 0.4 to 1, reflecting that the sorption was favourable. As shown in Figure 5, the hall parameters decreased when the initial concentrations increased. These results mean that the sorption was the most favourable at high initial concentration. On the other hand, the lowest values of the Hall parameters for the activated charcoal correlated well with the lowest values of the free Gibbs energy, indicating that the sorption of Cd and TCL on AC was more spontaneous and less reversible than the sorption process on WS and AWS.

Freundlich model

Freundlich isotherm model can be used for non-ideal sorption on heterogeneous surfaces and multilayer adsorption. This model is the earliest known empirical model which is shown to be stable with exponential distribution of active sites, characteristic of heterogeneous surfaces. The linear form of the Freundlich model is given by the following equation (5).

$$\ln(q_e) = \ln K_f + 1/n \ln(C_e), \qquad (5)$$

where q_e is the amount of pollutant adsorbed per g of support (mg g^{-1}), C_e represents the equilibrium concentration of the adsorbate material (mg L^{-1}). K_f and n are both the Freundlich constants. Kf is related to the relative adsorption capacity of the sorbent when the equilibrium concentration equals 1 mg L^{-1} and is a characteristic of the sorption system (adsorbent and adsorbate) ($mg^{1-(1/n)}$ $L^{1/n}$ g^{-1}) (Mallek et al., 2018) whereas n gives information about adsorption intensity (dimensionless).

Freundlich isotherms of Cd and TCL were presented in Figures 5A and 5B, respectively. Very good correlation coefficients were obtained for each modality, ranging from 0.969 to 0.996 (Table 6). Freundlich constants, K_f and n, were assessed from the origin intercept and the slope of the curves (Fig. 5A and 5B) as indicated by the linearized equation (5). As shown in Table 6, the relative sorption capacity of Cd on AC (Kf = 0.08) was lower than that on WS (Kf = 0.16) suggesting that AC is less efficient than WS to sorb Cd when the concentration of initial solution is 1 mg L^{-1}. This result needs to be considered with caution since Asuquo et al. (2017) demonstrated that the Langmuir isotherm is a better isotherm for the description of Cd on AC than the Freundlich isotherm. For TCL, this constant was equal (Kf = 0.17), suggesting the same efficacy of AC and AWS supports in the sorption of TCL at 1 mg L^{-1}. According to the study of Mallek et al. (2018), the n constant provides information about the intensity of the sorption. It can be considered as favourable ($2 < n < 10$), moderate ($1 < n < 2$) or difficult ($0 < n < 1$). In the current study, n was in the range 1 – 2, indicating that the intensity of the sorption of Cd and TCL on AC and WS/AWS was moderate (Table 6). Nevertheless, it is worth mentioning that the sorption intensity on the two studied supports seemed to be better for TCL than Cd.

Conclusion

Among the three sorbents studied, MB had the inconvenient of releasing intrinsic PAHs in filtrates. For ashes from R and WS, modeling isotherms revealed that: i) WS ashes were an excellent MTE extractor that exceeded the potential of well-known AC and ii) AR and AWS ashes were very effective in eliminating the selected EOCs displaying equipotent or superior activity compared to AC. Acidification of the sorbents allowed to modulate their affinity for targeted MTE or EOCs. Additional

efforts are now needed to study the retention capacity of combos of pollutants on these supports and to test the technology *in natura*.

Acknowledgments

The authors thank the Région Hauts-de-France and Yncréa Hauts-de-France for financial support (FEDER funding) of this work and technical help and facilities. The authors also acknowledge the spirulina powder producer La Spiruline de Marc, Saint-Léger-lès-Authie, France, for providing the wheat straw ashes.

Declaration of competing interest

The authors declare that they have no known competing financial interests or personal relationships that could have appeared to influence the work reported in this paper.

References

Ahsan, M.A., Islam, M.T., Imam, M.A., Hyder, A.H.M.G., Jabbari, V., Dominguez, N., Noveron, J.C., 2018. Biosorption of bisphenol A and sulfamethoxazole from water using sulfonated coffee waste: Isotherm, kinetic and thermodynamic studies. J. Environ. Chem. Eng. 6, 6602–6611.

Andersson, D.I., Hughes, D., 2012. Evolution of antibiotic resistance at non-lethal drug concentrations. Drug Resist. Updates 15, 162–172.

Asuquo, E., Martin, A., Nzerem, P., Siperstein, F., Fan X., 2017. Adsorption of Cd(II) and Pb(II) ions from aqueous solutions using mesoporous activated carbon adsorbent: Equilibrium, kinetics and characterization studies. J. Environ. Chem. Eng. 5, 679–698.

Bahar, M.M., Mahbub, K.R., Naidu, R., Megharaj, M., 2018. As(V) removal from aqueous solution using a low-cost adsorbent coir pith ash: Equilibrium and kinetic study. Environ. Technol. Innov. 9, 198–209.

Bhatnagar, A., Sillanpää, M., Witek-Krowiak, A., 2015. Agricultural waste peels as versatile biomass for water purification – A review. Chem. Eng. J. 270, 244–271.

329 Blázquez, G., Martín-Lara, M.A., Dionisio-Ruiz, E., Tenorio, G., Calero, M. 2012. Copper biosorption
330 by pine cone shell and thermal decomposition study of the exhausted biosorbent. J. Ind. Eng. Chem.
331 18, 1741–1750.
332 Boni, M.R., Chiavola, A, Marzedu, S. 2018. Application of biochar to the remediation of Pb-
333 contaminated solutions. Sustainability 10, 4440–1750.
334 Boni, M.R., Chiavola, A, Marzedu, S. 2020. Remediation of lead-contaminated water by virgin
335 coniferous wood biochar adsorbent: batch and column application. Water Air Soil Pollut. 231, 171–
336 187. Bonnefille, B., Gomez, E., Courant, F., Escande, A., Fenet, H., 2018. Diclofenac in the marine
337 environment: A review of its occurrence and effects. Mar. Pollut. Bull. 131, 496–506.
338 Burakov, A.E., Galunin, E.V., Burakova, I.V., Kucherova, A.E., Agarwal, S., Tkachev, A.G., Gupta,
339 V.K., 2018. Adsorption of heavy metals on conventional and nanostructured materials for wastewater
340 treatment purposes: A review. Ecotox. Environ. Safe. 148, 702–712.
341 Djelloul, K, 2014. Experimentation, modélisation et optimization de l'adsorption des effluents textiles.
342 Thesis, University Mohamed Khider De Briska, 116 pp.
343 Fernández-López, J.A., Angosto, J.M., Roca, M.J., Doval Miñarro, M., 2019. Taguchi design-based
344 enhancement of heavy metals bioremoval by agroindustrial waste biomass from artichoke. Sci. Total
345 Environ. 653, 55–63.
346 Fu, C., Zhang, H., Xia, M., Lei W., Wang, F., 2020. The single/co-adsorption characteristics and
347 microscopic adsorption mechanism of biochar-montmorillonite composite adsorbent for
348 pharmaceutical emerging organic contaminant atenolol and lead ions. Ecotox. Environ. Safe. 187,
349 109763.
350 Goulas, A., Louvel, B., Waterlot, C. 2015. Analytical method for determining polycyclic aromatic
351 hydrocarbon pollutants using ultra-fast liquid chromatography with fluorescence detection and the
352 new column packed with 5 µm Kinetex-C18 core-shell particles. Can. J. Chem. 93, 564–571.
353 Guo, X., Tian, B., Xin, L., (2013). Adsorption removal process and mechanism of diclofenac. Chinese
354 Journal of Environmental Engineering, 7(10), 3779–3784.
355 Gupta, V.K., Ali, I., 2000. Utilisation of bagasse fly ash (a sugar industry waste) for the removal of
356 copper and zinc from wastewater. Sep. Purif. Technol. 18, 131–140.

Gupta, V.K., Jain, C.K., Ali, I., Chandra, S., Agarwal, S., 2002. Removal of lindane and malathion from wastewater using bagasse fly ash-a sugar industry waste. Water Res. 36, 2483-2490.

Gupta, V.K., Jain, C.K., Ali, I., Sharma, M., Saini, V.K., 2003. Removal of cadmium and nickel from wastewater using bagasse fly ash—a sugar industry waste. Water Res. 37, 4038–4044.

Gupta, V.K., Mohan, D., Sharma, S., Sharma, M., 2000. Removal of Basic Dyes (Rhodamine B and Methylene Blue) from Aqueous Solutions Using Bagasse Fly Ash. Sep. Sci. Technol. 35, 2097–2113.

Hamdaoui, O., Naffrechoux, E., 2007. Modeling of adsorption isotherms of phenol and chlorophenols onto granular activated carbon Part I. Two-parameter models and equations allowing determination of thermodynamic parameters. J. Hazard. Mater. 147, 381–394

Jackson, L.M., Felgenhauer, B.E., Klerks, P.L., 2019. Feminization, altered gonadal development, and liver damage in least killifish (Heterandria formosa) exposed to sublethal concentrations of 17α-ethinylestradiol. Ecotox. Environ. Safe. 170, 331–337.

Janus, A., Pelfrêne, A., Sahmer, K., Heymans, S., Deboffe, C., Douay, F., Waterlot, C., 2017. Value of biochars from Miscanthus x giganteus cultivated on contaminated soils to decrease the availability of metals in multicontaminated aqueous solutions. Environ. Sci. Pollut. Res. 24, 18204–18217.

Jean, J., Perrodin, Y., Pivot, C., Trepo, D., Perraud, M., Droguet, J., Tissot-Guerraz, F., Locher, F., 2012. Identification and prioritization of bioaccumulable pharmaceutical substances discharged in hospital effluents. J. Environ. Manage. 103, 113–121.

Jeirani, Z., Hui Niu, C., Soltan, J., 2017. Adsorption of emerging pollutants on activated carbon. Rev. Chem. Eng. 33, 491–522.

Lapworth, D.J., Baran, N., Stuart, M.E., Ward, R.S., 2012. Emerging organic contaminants in groundwater: A review of sources, fate and occurrence. Environ. Pollut. 163, 287–303.

Li, J., Jiang, L., Xiang, X., Xu, S., Wen, R., Liu, X., 2013. Competitive sorption between 17α-ethinyl estradiol and bisphenol A /4-n-nonylphenol by soils. J. Environ. Sci. 25, 1154–1163.

Liu, X., Ji, R., Shi, Y., Wang, F., Chen W., 2019. Release of polycyclic aromatic hydrocarbons from biochar fine particles in simulated lung fluids: Implications for bioavailability and risks of airborne aromatics. Sci. Total. Environ. 655, 1159–1168.

384 Luo, M., Lin, H., Li, B., Dong, Y., He, Y., Wang, L., 2018. A novel modification of lignin on
385 corncob-based biochar to enhance removal of cadmium from water. Biores. Technol. 259, 312–318.
386 Naga Babu, A., Reddy, D.S., Kumar, G.S., Ravindhranath, K., Krishna Mohan, G.V., 2018. Removal
387 of lead and fluoride from contaminated water using exhausted coffee grounds based bio-sorbent. J.
388 Environ. Manage. 218, 602–612.
389 Mallek, M., Chtourou, M., Portillo, M., Monclús, H., Walha, K., Salah, A. ben, Salvadó, V., 2018.
390 Granulated cork as biosorbent for the removal of phenol derivatives and emerging contaminants. J.
391 Environ. Manage. 223, 576–585.
392 Qasemi, M., Afsharnia, M., Zarei, A., Najafpoor, A.A., Salari, S., Shams, M., 2018. Phenol removal
393 from aqueous solution using Citrullus colocynthis waste ash. Data in Brief 18, 620–628.
394 Rodriguez-Narvaez, O.M., Peralta-Hernandez, J.M., Goonetilleke, A., Bandala, E.R., 2017. Treatment
395 technologies for emerging contaminants in water: A review. Chem. Eng. J. 323, 361–380.
396 Santos, J.L., Aparicio, I., Alonso, E., 2007. A new method for the routine analysis of LAS and PAH in
397 sewage sludge by simultaneous sonication-assisted extraction prior to liquid chromatographic
398 determination. Anal. Chim. Acta. 605, 102–107.
399 Savio, M., Cerutti, S., Martinez, L.D., Smichowski, P., Gil, R.A., 2010. Study of matrix and spectral
400 interferences in the determination of lead in sediments, sludges and soils by SR-ETAAS using slurry
401 sampling. Talanta 82, 523–527.
402 Sophia, A.C., Lima, E.C., 2018. Removal of emerging contaminants from the environment by
403 adsorption. Ecotox. Environ. Safe. 150, 1–17.
404 Sun F., Littlejohn, D., Gibson, M.D., 1998. Ultrasonication extraction and solid phase extraction
405 clean-up for determination of US EPA 16 priority pollutant polycyclic aromatic hydrocarbons in soils
406 by reversed-phase liquid chromatography with ultraviolet absorption detection. Anal. Chim. Acta. 364,
407 1–11.
408 Sun K., Jin, J., Gao, B., Zhang, Z.-Y., Wang, Z., Pan, Z.-Z., Xu, D., Zhao, Y., 2012. Sorption of 17α-
409 ethinyl estradiol, bisphenol A and phenanthrene to different size fractions of soil and sediment.
410 Chemosphere 88, 577–583.

411 Thomaidi, V.S., Matsoukas, C., Stasinakis, A.S., 2017. Risk assessment of triclosan released from
412 sewage treatment plants in European rivers using a combination of risk quotient methodology and
413 Monte Carlo simulation. Sci. Total Environ. 603–604, 487–494.
414 Tirkey, P., Bhattacharya, T., Chakraborty, S., 2018. Optimization of fluoride removal from aqueous
415 solution using Jamun (Syzygium cumini) leaf ash. Process Safe. Environ. Protect. 115, 125–138.
416 Tomczyk, A., Sokolowska, Z., Boguta, P., 2020. Biochar Physicochemical properties: pyrolysis
417 temperature and feedstock kind effects. Rev. Environ. Sci. Bio. 19, 191–225.
418 Trigo, C., Spokas, K. A., Cox, L., & Koskinen, W. C., 2014. Influence of soil biochar aging on
419 sorption of the herbicides MCPA, nicosulfuron, terbuthylazine, indaziflam, and
420 fluoroethyldiaminotriazine. J. Agri. Food. Chem. 62, 10855–10860.
421 Tursi, A., Beneduci, A., Chidichimo, F., De Vietro, N., Chidichimo, G., 2018. Remediation of
422 hydrocarbons polluted water by hydrophobic functionalized cellulose. Chemosphere 201, 530–539.
423 Wang, C., Liang, S., Zhang, Y., 2018. The ecological competition and grazing reverse the effects of
424 sulfamethoxazole on plankton: a case study on characterizing community-level effect. Environ. Sci.
425 Pollut. Res. 25, 17283–17288.
426 Wang, C., Odinga, E.S., Zhang, W., Zhou, X., Yang, B., Waigi, M.G., Gao, Y., 2019. Polyaromatic
427 hydrocarbons in biochars and human health risks of food crops grown in biochar-amended soils: A
428 synthesis study. Environ. Int. 130, 104899.
429 Waterlot, C., Bidar, G., Pruvot, C., Douay F., 2011. Analysis of cadmium in water extracts from
430 contaminated soils with high arsenic and iron concentration levels. J. Environ. Sci. Eng. 5, 271–280.
431 Waterlot, C., Douay, F., 2009. The problem of arsenic interference in the analysis of Cd to evaluate its
432 extractability in soils contaminated by arsenic. Talanta 80, 716–722.
433 Waterlot, C., Goulas, A., 2016. Temperature effects on retention and separation of PAHs in reversed-
434 phase liquid chromatography using columns packed with fully porous and core-shell particles. J.
435 Chem-ny 12 pages.
436 Waterlot, C., Hechelski, M., 2019. Benefits of ryegrass on multicontaminated soils. Part 1: Effects of
437 fertilizers on bioavailability and accumulation of metals. Sustainability 11, 5093-6013.

438 Zaltauskaite, J., Miskelyte, D., 2018. Biochemical and life cycle effects of triclosan chronic toxicity to
439 earthworm Eisenia fetida. Environ. Sci. Pollut. Res. 25, 18938–18946.
440 Zhou, J., Chen, H., Huang, W., Arocena, J.M., Ge, S., 2016. Sorption of atrazine, 17-α-estradiol, and
441 phenanthrene on wheat straw and peanut shell biochars. Water Air Soil Pollut. 227, 1–13.
442 Żółtowska-Aksamitowska, S., Bartczak, P., Zembrzuska, J., Jesionowski, T., 2018. Removal of
443 hazardous non-steroidal anti-inflammatory drugs from aqueous solutions by biosorbent based on chitin
444 and lignin. Sci. Total Environ. 612, 1223–1233.
445

446 **Table 1**. Structure, physicochemical properties and pictograms of the studied MTE and EOCs

447 pollutants

448

	Chemical Structure	MW[a] (g mol^{-1})	Water solubility (mg L^{-1})	Log K_{ow}[b]	Pictogram
DCF		296.15	2.37	4.51	
SFX		253.28	610	0.89	
EE2		296.41	11.3	3.67	
TCL		289.54	10	4.76	
Cd	-	112.41	-	-	
Pb	-	207.20	-	-	

449 DCF: diclofenac; SFX: sulfamethoxazole; EE2: 17α-ethinylestradiol; TCL: triclosan; Cd: cadmium;

450 Pb: lead.

451 [a] Molecular weight;

452 [b] Log octanol-water partition coefficient.

453

Table 2: UFLC analyses: composition of the mobile phase, λ_{max}, retention time, limits of detection and quantification for each organic pollutant

	CH_3CN/H_2O (%)	Flow rate (mL min^{-1})	λ_{max} (nm)	Retention time (min)	LD[a] (mg L^{-1})	LQ[b] (mg L^{-1})
SFX	30/70	0.8	267	3.070	0.0026	0.0079
TCL	20/80	0.8	280	5.561	0.0448	0.1345
EE2	20/80	0.8	282	3.664	0.3181	0.9542
DCL	10/90	0.8	277	3.594	n.d	n.d

[a] limit of detection; [b] limit of quantification ; n.d.: no determined

Table 3: Concentration of metals in solution after filtration of artificially contaminated water ([metal] or [organic pollutant] = 20 mg L^{-1}, V = 25 mL, mass of support = 1 g) on miscanthus biochar (MB)

[Cd] (mg L^{-1})	[Pb] (µg L^{-1})	[TCL] (mg L^{-1})	[EE2] (mg L^{-1})	[SFX] (mg L^{-1})	[DCF] (mg L^{-1})
16.95	52.7	2.47	19.5	20	20

Indicated values are the mean of two independent experiments.

Table 4: Residual concentration of filtrates after filtration of contaminated solutions (at 20 mg L^{-1}) using 1 g of solid support

Support	[Cd] mg L^{-1}	[Pb] mg L^{-1}
AC	0.00420	0.0492
R	0.00525	0.101
WS	<LD*	0.0362
AR	4.29	12.60
AWS	17.60	6.88

* LD = 0.0021 µg L^{-1}

AC=activated charcoal Norit® SA-2; R=ryegrass ashes; WS= wheat straw ashes; AR=acidified ryegrass ashes; ACS=acidified wheat straw ashes.

Indicated values are the mean of two independent experiments.

480 **Table 5**: Residual concentration in solutions after their filtration using 1 g of solid support

Support	EE2 (mg L^{-1})	TCL (mg L^{-1})	SFX (mg L^{-1})	DCF (mg L^{-1})
AC	0.508	0.073	0.016	<LD
R	20	20	<LD	20
WS	17	13.915	15.65	20
AR	18.135	2.690	1.835	<LD
AWS	11.235	<LD	<LD	<LD

481 AC=activated charcoal Norit® SA-2; R=ryegrass ashes; WS= wheat straw ashes; AR=acidified
482 ryegrass ashes; ACS=acidified wheat straw ashes.
483 Indicated values are the mean of two independent experiments.
484

485 **Table 6**: Langmuir and Freundlich constants of Cd and TCL sorption on AC and WS/AWS

Pollutant	Support	Langmuir constants			Freundlich constants		
		q_m ($mg\ g^{-1}$)	b ($L\ mg^{-1}$)	R^2	K_f *	n	R^2
Cd	AC	145.5	7.23E-04	0.993	0.08	1.01	0.983
	WS	529.1	1.87E-04	0.996	0.16	1.09	0.996
TCL	AC	6.36	1.81E-02	0.975	0.17	1.35	0.975
	AWS	16.6	6.44E-03	0.996	0.17	1.26	0.969

486

487 * Unit of K_f is $mg^{1-(1/n)}\ L^{1/n}\ g^{-1}$

488 AC=activated charcoal Norit® SA-2; WS= wheat straw ashes; ACS=acidified wheat straw ashes.

489

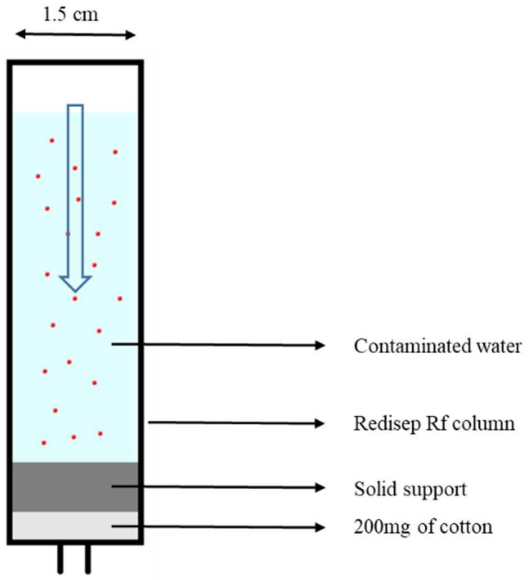

Figure 1: Lab-engineered cartridge filtration system

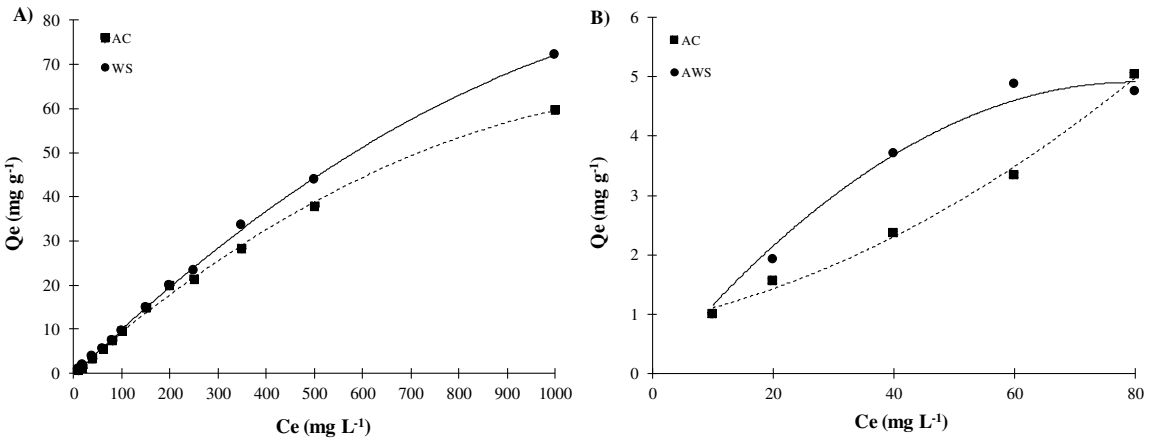

Figure 2: Sorption isotherm of Cd (A) and TCL (B) on AC and WS/AWS

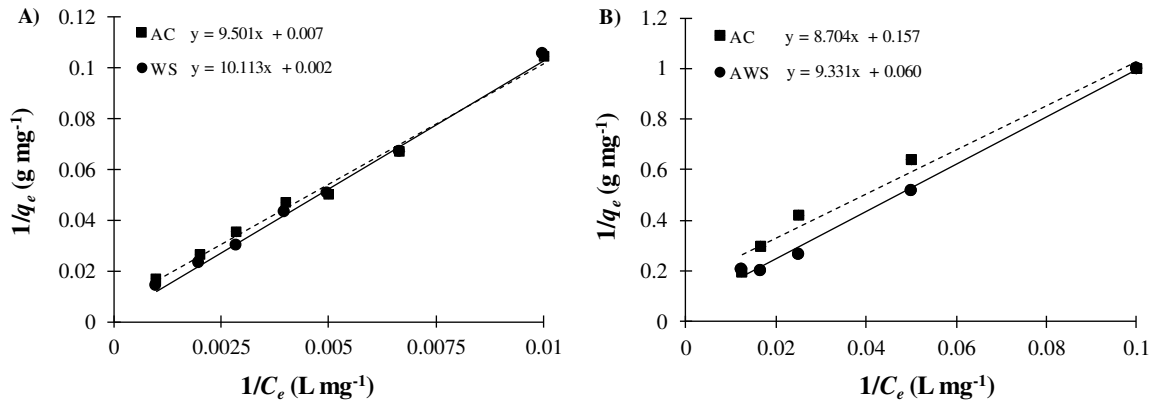

Figure 3: Langmuir isotherm on AC and WS/AWS; A) Cd and B) TCL

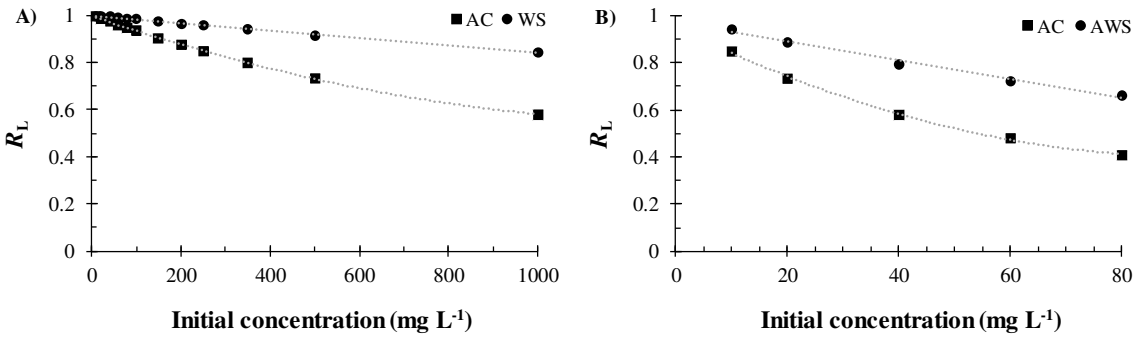

Figure 4: Variation of the Hall parameter; A) Cd and B) TCL

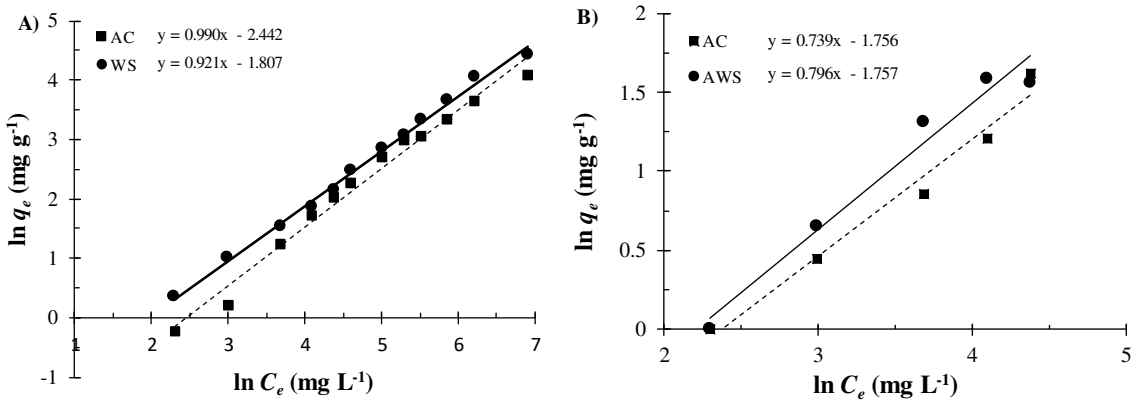

Figure 5: Freundlich isotherm on AC and WS/AWS; A) Cd and B) TCL

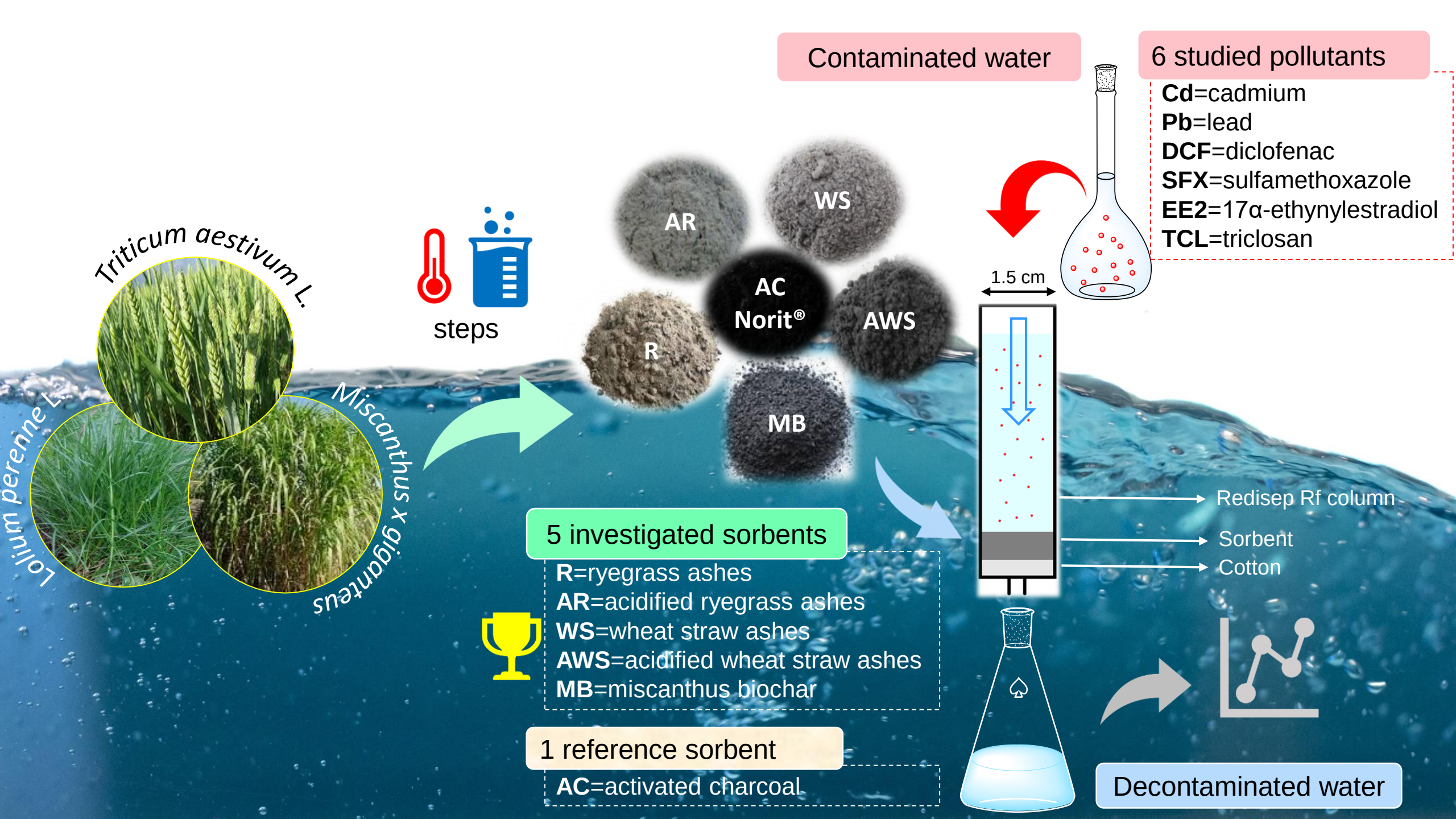
Contaminated water
6 studied pollutants
Cd=cadmium
Pb=lead
DCF=diclofenac
SFX=sulfamethoxazole
EE2=17α-ethynylestradiol
TCL=triclosan
Triticum aestivum L.
Lolium perenne L.
Miscanthus x giganteus
steps
AR
WS
AC
Norit®
AWS
R
MB
1.5 cm
Redisep Rf column
Sorbent
Cotton
5 investigated sorbents
R=ryegrass ashes
AR=acidified ryegrass ashes
WS=wheat straw ashes
AWS=acidified wheat straw ashes
MB=miscanthus biochar
1 reference sorbent
AC=activated charcoal
Decontaminated water